Exercise 4 - Solution

April 11, 2025

LTE, EPFL, Switzerland

Question 1

SEVIRI measures outwelling radiation from the Earth at different wavelengths. The principle is thus similar to the one of LandSat (exercise 3), but the wavelengths are different (mainly in the infrared). The outwelling radiation is the sum of reflected sun radiation and the direct emission from objects on Earth or in the atmosphere. The emission spectrum of an object (intensity of the radiation it produces, as a function of wavelength) depends on its composition and on its temperature. The radiation in a infrared is more intense for an object with high temperature. For the detection of clouds, reflectance and emission in visible and near-infrared are useful. In the case of a homogeneous cloud, the thermal infrared channels can be used as a qualitative indicator of cloud top height: colder temperatures are related to a higher cloud top.

Question 2

Most of sunlight's intensity is in the range of visible wavelengths (see example). In this range, the effect of clouds is mostly related to their albedo: the outwelling radiation is largely the reflection of the sun light. Because they reflect so much of this energy, they appear as white (high intensity pixels) in the images.

In the infrared, the direct emission of the objects becomes more important. In the temperature range of objects on Earth, the black body spectrum is mainly in the infrared. Conversely, the intensity of sunlight in this range is not as important as in the visible range. The intensity of a pixel is therefore related to the temperature of the object. Since clouds are at a higehr altitude than the surface, they have a lower temperature than the surface, and appear as low-intensity (black) pixels.

Question 3

The brightest area at this timestep is shown in Figure 1. It suggests that this spot has a higher temperature than the surroundings. It corresponds to the Rhone valley, in the

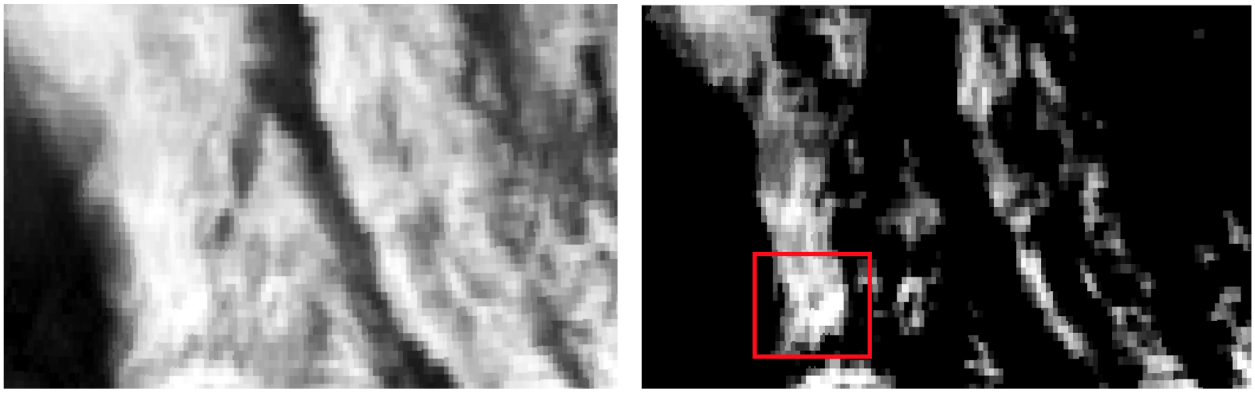

Figure 1: IR134 SEVIRI image at 14:00 UTC (*IR_134/201906151400_SEVIRI_IR_134.tiff*)

canton of Valais, between Sion and Martigny, an area which typically features high temperatures in summer. In Figure 1, the sharp angle of the Rhone valley close to Martigny is visible. To visualize better the brightest areas, the color scale was adjusted.

Question 4

We chose to use thresholds on the VIS_006 and the IR_039 channels to identify the clouds (here, pixels with VIS_006 $>$ 80 and IR_039 $<$ 150 are displayed). In the Raster calculator, a layer was created with the following formula:

```
"201906151400_SEVIRI_IR_087@1"*("201906151400_SEVIRI_VIS006@1">80
AND "201906151400_SEVIRI_IR_039@1"<150)
```

This is an example of solution; other thresholds can be used.

A singleband pseudocolor colormap was then chosen to better highlight the differences in the observed clouds. In Figure 2, three clouds can be seen; the leftmost with pixel values mostly in the 0-25 range; the middle one in the 25-75 range; and the last one largely $>$ 75. Therefore, assuming they have relatively similar composition (and hence radiative properties), the three clouds (from left to right) have increasing temperatures, which in turn suggests they have decreasing cloud top heights.

Question 5

Since channel IR134 is the furthest from the visible range in the provided data, it is well-suited to evaluate temperatures (less of the outwelling radiation at this wavelength is reflected sunlight).

In Figure 3, the colorbar was adjusted to highlight the pixels with the lowest intensity, i.e. with coldest temperature in the storm cloud. This indicates the position of the highest parts of the storm cloud (the overshooting top). We can expect the strongest precipitation to occur close to those points.

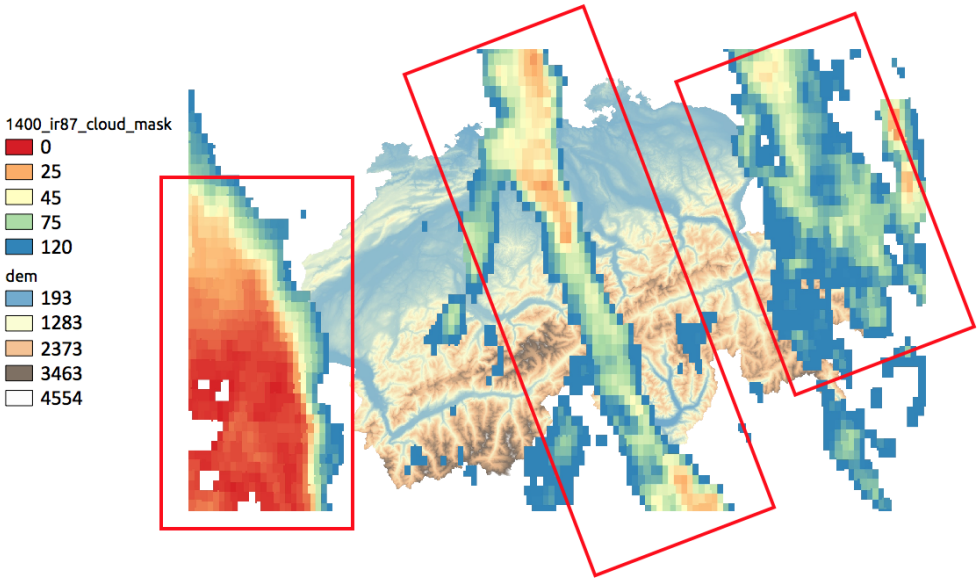

Figure 2: Different types of clouds over Switzerland at 1400 on 15/06/2019.

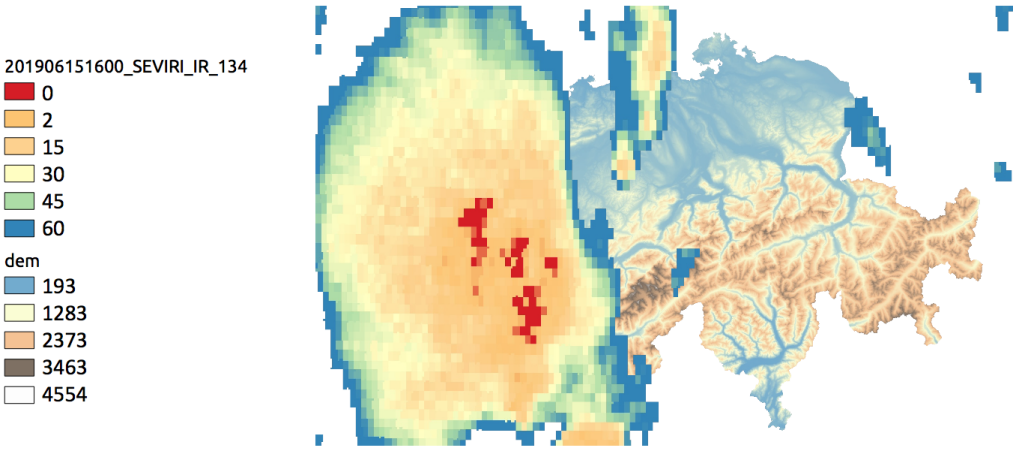

Figure 3: Storm cloud in IR 134. The color scale is chosen to show location of coldest temperatures

Another method can be used to highlight the cloud top, based on a normalized difference index (similar to Lab 3). Using $NDI = \frac{IR_{134}-IR_{39}}{IR_{134}+IR_{39}}$, i.e. the two most extreme IR values that we have, we obtain Figure 4, where the minimum value corresponds to the highest cloud top.

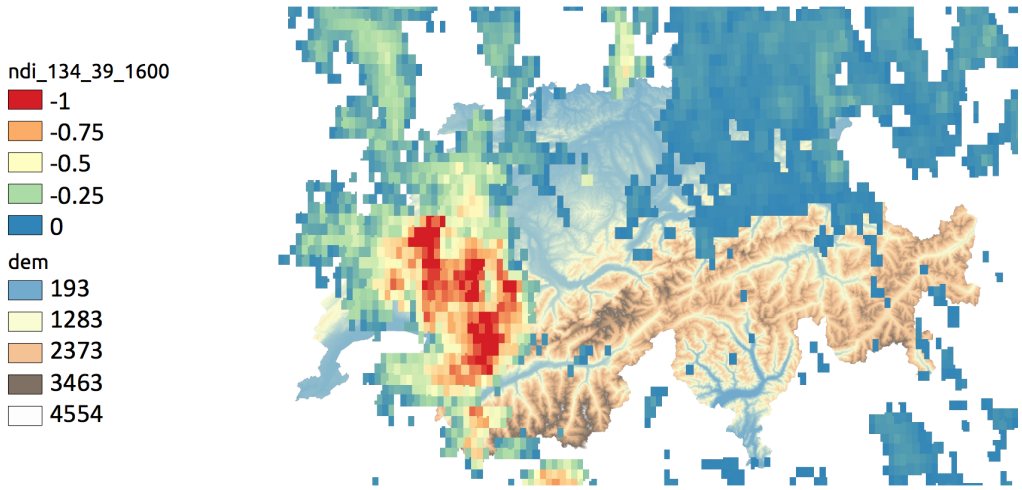

Figure 4: Normalized difference index (NDI) 134-39, at 1600 UTC. The color scale is chosen to show location of coldest temperatures, i.e. with smallest NDI, and values > 0 are set to transparent

Question 6

Both CombiPrecip and RZC show that, at 16:00 UTC, the highest rain rates of the main storm are found in the Plateau and in the Prealps, i.e. in the area circled in white in Figure 5. This is close to the low-intensity pixels from SEVIRI IR134 (i.e. cloud top); actually, the strongest precipitation intensity appears to be right behind the overshooting cloud top. Looking at Figure 1 from the exercise, we see that the overshooting top is rather indicative of the updraft location, while the precipitation peak is in the downdraft area. This might not always be visible when looking at IR and radar data, and should be interpreted with care: because of the storm's horizontal motion, precipitation is advected horizontally while it falls and thus the peak precipitation is not just below the start of the downdraft, which is high up in altitude).

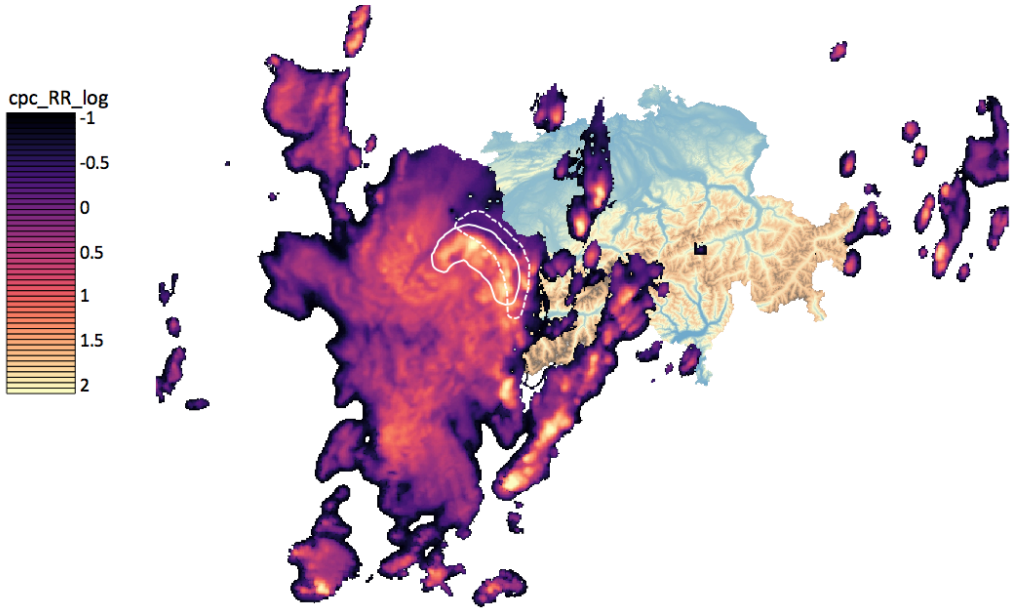

Figure 5: Rain rate from Combiprecip (log10). The area circled in full white is where the strongest precipitation intensities are estimated (in Switzerland) for this timestep. The dashed white line indicates where the minimum pixel values were seen in question 5 (SEVIRI data).

Question 7

Figure 6 shows the difference in the logarithms of Combiprecip and RZC rain rates. By visualizing the difference in the logarithms, we focus on the ratio between Combiprecip and RZC. Two main differences are seen:

1. The red area surrounding the precipitation field. There, Combiprecip shows more precipitation than RZC. This can be related to Combiprecip producing a smoother precipitation field than RZC: the edges of the precipitation area are less clear-cut, meaning there are entire zones where virtually no precipitation is detected by the RZC algorithm, while Combiprecip predicts some, which leads to a large Combiprecip/RZC ratio.

2. Even more striking are the blue spots, where Combiprecip has much less precipitation than RZC ($log(CPC) - log(RZC) \sim -2$, i.e. RZC is 100 times more than CPC). Those spots are quite local, which suggests that they are related to the rain gauge measurements incorporated by CPC. In fact, upon closer inspection, it can be seen that the blue spots are exactly at the location of some rain gauges or weather stations. In these places, the radar-derived estimations are therefore far off from the rain gauges measurements. It should be kept in mind that rain gauges themselves are subject to uncertainty, especially in strong wind events: since the pluviometers are not shielded from the wind, they can underestimate precipitation. In such cases, it is difficult to know the ground truth.

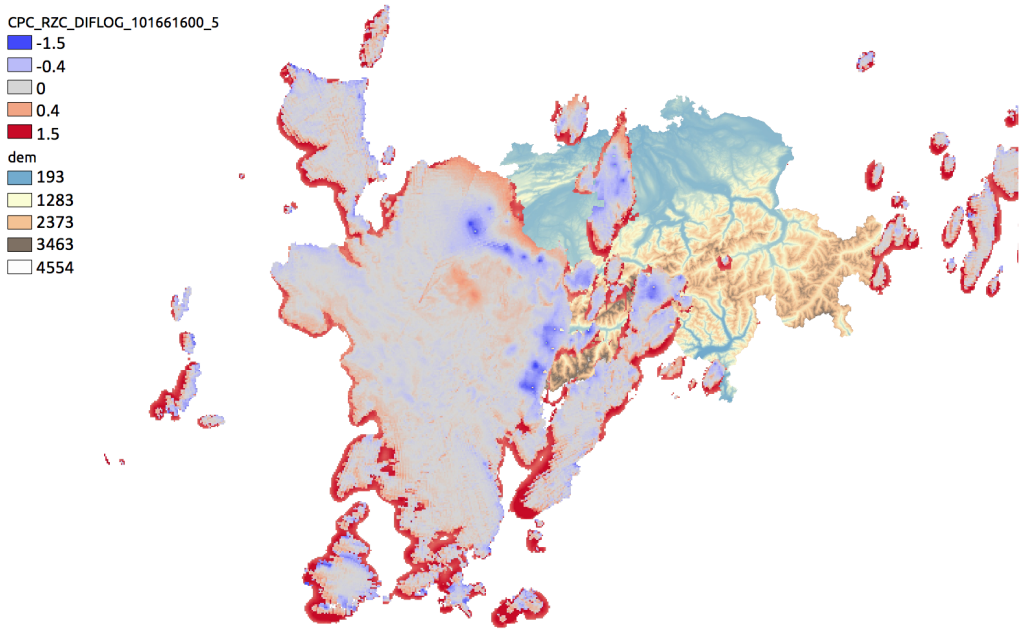

Figure 6: Difference in $log_{10}(CPC)$ and $log_{10}(RZC)$.

By looking at the difference in the Combiprecip and RZC values (the linear difference in the precipitation estimates, Figure 7), we look at a more physically relevant quantity (uncertainty in the rainfall at a given location). The striking feature in this difference is that RZC underestimates Combiprecip close to the area with the strongest precipitation.

The difference is up to 15 mm/h, which is a significant bias. Outside of this area, the difference is small, even though the ratio of Combiprecip and RZC estimates can be large.

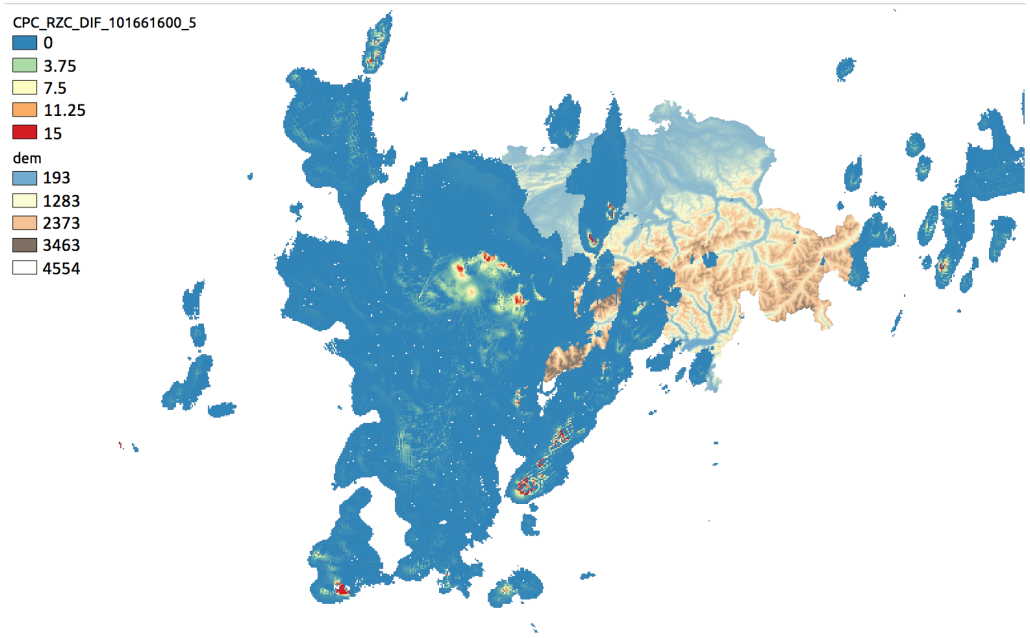

Figure 7: Difference in CPC and RZC (in mm/h)

Question 8

Close to the radar, a line can be drawn along the zero-velocity pattern (see Figure 8). In this zone, it means that the direction of the scatterers is perpendicular to the radar beam. The wind direction is therefore given by the perpendicular to this line. Since negative velocity indicates motion toward the radar, the conclusion is that the wind is South-West (blowing from $120°$).

To find the wind speed, we look at the Doppler velocity values where the radar beam is parallel to the wind direction (see Figure 8). The estimate we obtain is about 12 m/s (43 km/h).

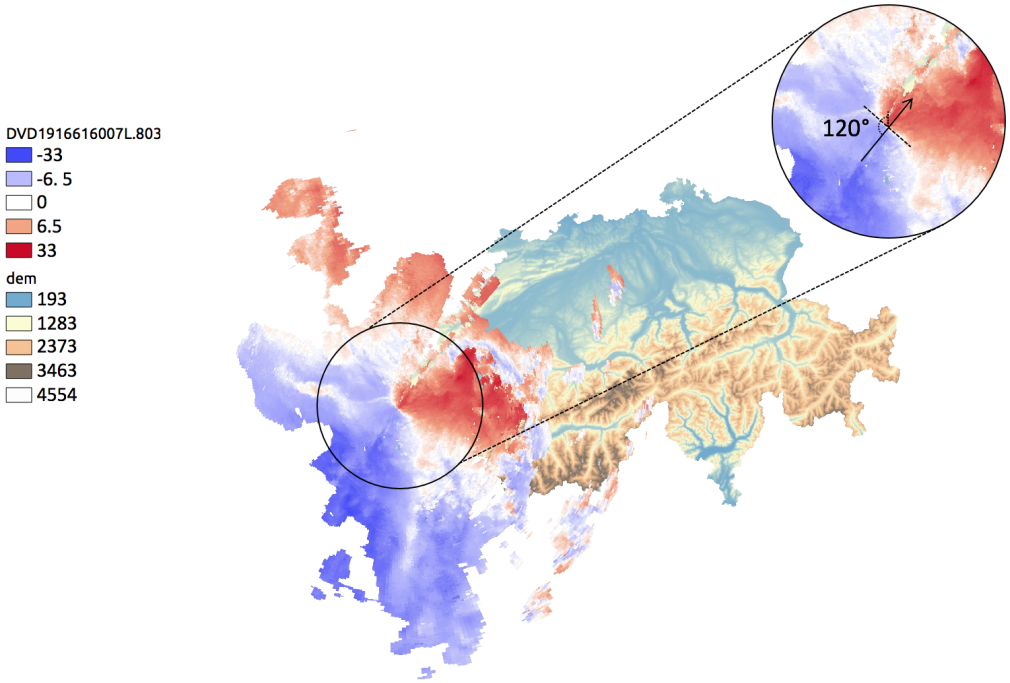

Figure 8: Interpreting the wind direction from the Doppler pattern.

Question 9

A sharp slice of the radar measurements is virtually empty, to the North-East of the radar. This is also visible in the Combiprecip and RZC data, with a discontinuity at this location. This is an artifact due to beam blockage very close to the radar. When looking at the aerial view of the La Dôle radar, it can be seen that a larger building is located close to the radar (see Figure 9). This is the Skyguide radar (dedicated to aircraft): being so close to the MeteoSwiss radar, it prevents it from scanning in a range of a few degrees in azimuth. This deteriorates the precipitation estimation in the area not covered by the scans.

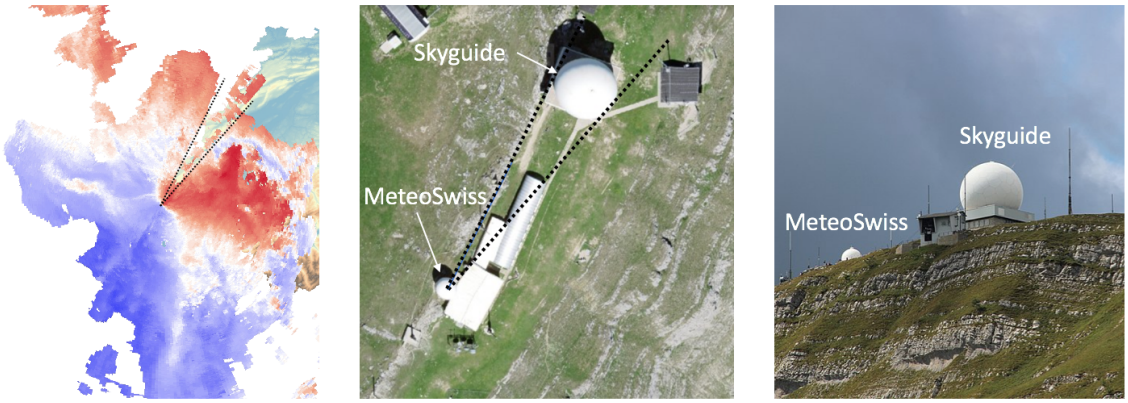

Figure 9: Beam blockage at the La Dôle radar due to Skyguide.

Question 10

At the front of the storm cloud, signatures of physical processes are visible in satellite and radar data.

1. Infrared imagery suggests the presence of a high (overshooting) cloud top, as detailed in question 5 (dashed contour in Figure 10).

2. Rain-rate products derived from measurements of radar equivalent reflectivity show a maximum close to this high cloud top (full contour in Figure 10).

3. The Doppler field goes quite abruptly from positive to negative velocity (see on Figure 10, in the same area as maximum precipitation). This means there is a motion of scatterers (hydrometeors) toward the radar, while the dominant motion of the storm in this location is away from the radar. Schematically, the negative velocities are a signature of the inflow of the thunderstorm (updrafts in the direction opposite to storm motion, red arrows in Figure 1 of the exercise PDF) while the enhanced positive velocities (dark red) show the outflow (downdrafts of cold air, blue arrows in Figure 1 of the exercise PDF).

Note that an exact comparison of the location of the Doppler velocity vs. rain-rate and IR signatures is not immediate, because the PPI is performed at an angle different than 0. In our case, at 0.93° of elevation, this has a relatively minor impact on the horizontal

distance to the radar (because $cos(1°) \approx 1$). However, the Doppler velocity values are not those at ground level: for example, 50 km away from the radar, the beam is at $50 \times sin(0.93°) \approx 0.8$ km above the radar altitude (neglecting both beam and Earth curvature).

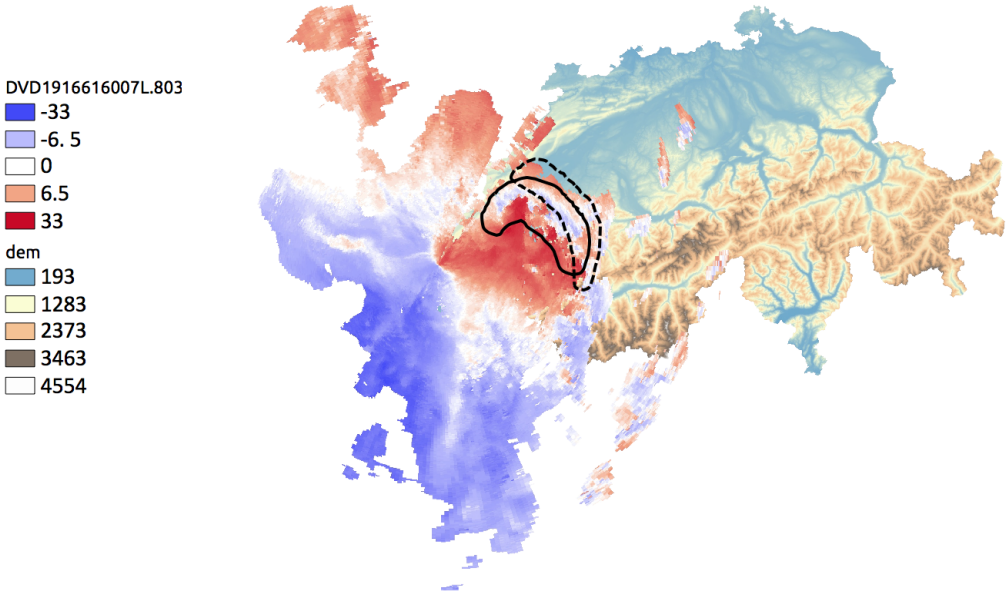

Figure 10: Analysis of Doppler field close to precipitation maximum